Flight-Propulsion Response Requirements for Directional Stability and Control

Nhan Nguyen*
NASA Ames Research Center, Moffett Field, CA 94035
Vahram Stepanyan†
SGT/NASA Ames Research Center, Moffett Field, CA 94035

I. Introduction

The vertical stabilizer is a primary aerodynamic surface responsible for providing directional stability of an aircraft. Directional stability is further augmented by the yaw damping capability of the rudder using feedback control. When the rudder experiences faults or the vertical stabilizer is damaged, directional stability of an aircraft will be compromised. In the worst-case scenario, the vertical stabilizer would become completely separated that would cause a loss of control. While rare, this occurrence was a causal factor for the crash of the American Flight 587 in 2001.[1] In an event that directional stability of an aircraft is compromised, aircraft engines can potentially be used in an autopilot mode to regain aircraft stability. The use of engine differential thrust for directional control has been demonstrated by the United Flight 132 accident in Sioux City, Iowa, in 1989[2] and the DHL incident in Baghdad, Iraq, in 2003.[3] As a control actuator, aircraft engines are generally slower than the conventional flight control actuators, and therefore may not be able to respond quickly to changes in aircraft dynamics in order to maintain aircraft stability. In order to integrate aircraft engines into a flight control systems, aircraft engines would need to have a faster response time as well as additional thrust capability. This study examines the engine response time requirements in severe damage situations associated with the vertical stabilizer of a generic transport aircraft. The results of the study could be used to assess requirements for engine design for fast response in an emergency situation.

II. Flight Dynamics with Propulsion Control

Assuming that the aircraft is equipped with two symmetrically wing-mounted engines whose thrust lines are aligned with the fuselage centerline, then the full 6-dof nonlinear equations of motion for an aircraft subject to a C.G. coordinate shift by $(\Delta x, \Delta y, \Delta z)$ are given by

$$\begin{aligned}\dot{V} = {} & \frac{(T_L+T_R)\cos\alpha\cos\beta - C_D\bar{q}S\cos\beta + C_Y\bar{q}S\sin\beta}{m} + \cos\alpha\cos\beta\left[\left(q^2+r^2\right)\Delta x - (pq-\dot{r})\Delta y - (\dot{q}+pr)\Delta z\right] \\ & + \sin\beta\left[-(pq+\dot{r})\Delta x + \left(p^2+r^2\right)\Delta y - (qr-\dot{p})\Delta z\right] + \sin\alpha\cos\beta\left[-(pr-\dot{q})\Delta x - (qr+\dot{p})\Delta y + \left(p^2+q^2\right)\Delta z\right] \\ & - g\left(\cos\alpha\cos\beta\sin\theta - \sin\beta\cos\theta\sin\phi - \sin\alpha\cos\beta\cos\theta\cos\phi\right) \end{aligned} \tag{1}$$

$$\begin{aligned}\dot{\alpha} = {} & -\frac{(T_L+T_R)\sin\alpha + C_L\bar{q}S}{mV\cos\beta} + q - \tan\beta\left(p\cos\alpha + r\sin\alpha\right) - \frac{\cos\alpha\left[(pr-\dot{q})\Delta x + (qr+\dot{p})\Delta y - \left(p^2+q^2\right)\Delta z\right]}{V\cos\beta} \\ & - \frac{\sin\alpha\left[\left(q^2+r^2\right)\Delta x - (pq-\dot{r})\Delta y - (\dot{q}+pr)\Delta z\right]}{V\cos\beta} + \frac{g\left(\cos\alpha\cos\theta\cos\phi + \sin\alpha\sin\theta\right)}{V\cos\beta} \end{aligned} \tag{2}$$

*Research Scientist, Intelligent Systems Division, Mail Stop 269-1, AIAA Associate Fellow
†Research Scientist, Intelligent Systems Division, Mail Stop 269-1, AIAA Senior Member

$$\dot{\beta} = -\frac{(T_L+T_R)\cos\alpha\sin\beta - C_D\bar{q}S\sin\beta - C_Y\bar{q}S\cos\beta}{mV} - r\cos\alpha + p\sin\alpha$$
$$-\frac{\cos\alpha\sin\beta\left[\left(q^2+r^2\right)\Delta x-(pq-\dot{r})\Delta y-(\dot{q}+pr)\Delta z\right]}{V} - \frac{\cos\beta\left[(pq+\dot{r})\Delta x-\left(p^2+r^2\right)\Delta y+(qr-\dot{p})\Delta z\right]}{V}$$
$$+\frac{\sin\alpha\sin\beta\left[(pr-\dot{q})\Delta x+(qr+\dot{p})\Delta y-\left(p^2+q^2\right)\Delta z\right]}{V}$$
$$+\frac{g\left(\cos\alpha\sin\beta\sin\theta+\cos\beta\cos\theta\sin\phi-\sin\alpha\sin\beta\cos\theta\cos\phi\right)}{V} \tag{3}$$

$$\bar{I}_{xx}\dot{p}-\bar{I}_{xy}\dot{q}-\bar{I}_{xz}\dot{r}+\bar{I}_{xy}pr-\bar{I}_{xz}pq+\left(\bar{I}_{zz}-\bar{I}_{yy}\right)qr+\bar{I}_{yz}\left(r^2-q^2\right)=\bar{C}_l\bar{q}Sb \tag{4}$$
$$-\bar{I}_{xy}\dot{p}+\bar{I}_{yy}\dot{q}-\bar{I}_{yz}\dot{r}+\bar{I}_{yz}pq-\bar{I}_{xy}qr+\left(\bar{I}_{xx}-\bar{I}_{zz}\right)pr+\bar{I}_{xz}\left(p^2-r^2\right)=\bar{C}_m\bar{q}S\bar{c}+\left(T_L+T_R\right)z_e \tag{5}$$
$$-\bar{I}_{xz}\dot{p}-\bar{I}_{yz}\dot{q}+\bar{I}_{zz}\dot{r}+\bar{I}_{xz}qr-\bar{I}_{yz}pr+\left(\bar{I}_{yy}-\bar{I}_{xx}\right)pq+\bar{I}_{xy}\left(q^2-p^2\right)=\bar{C}_n\bar{q}Sb+\left(T_L-T_R\right)y_e \tag{6}$$

where T_L and T_R are the left and right engine thrusts, and $\bar{C}_l$, $\bar{C}_m$, and $\bar{C}_n$ are the moment coefficients defined as

$$\bar{C}_l = C_l - C_z\frac{\Delta y}{b} + C_y\frac{\Delta z}{b} \tag{7}$$
$$\bar{C}_m = C_m + C_z\frac{\Delta x}{\bar{c}} - C_x\frac{\Delta z}{\bar{c}} \tag{8}$$
$$\bar{C}_n = C_n - C_y\frac{\Delta x}{b} + C_x\frac{\Delta y}{b} \tag{9}$$
$$C_x = \frac{T_L+T_R}{\bar{q}S} + C_L\sin\alpha - C_D\cos\alpha\cos\beta \tag{10}$$
$$C_y = C_Y - C_D\sin\beta \tag{11}$$
$$C_z = -C_L\cos\alpha - C_D\sin\alpha\cos\beta \tag{12}$$

For small angles, the linearized equations of motion are obtained as

$$\frac{\bar{I}_{xx}\dot{p}-\bar{I}_{xy}\dot{q}-\bar{I}_{xz}\dot{r}}{\bar{q}Sb} = \bar{C}_{l_p}\frac{pb}{2\bar{V}} + \bar{C}_{l_q}\frac{q\bar{c}}{2\bar{V}} + \bar{C}_{l_r}\frac{rb}{2\bar{V}} + \left(C_{l_V}+2C_l\right)\frac{\Delta V}{\bar{V}} + \bar{C}_{l_\alpha}\Delta\alpha + \bar{C}_{l_\beta}\Delta\beta + \bar{C}_{l_{\dot{\alpha}}}\frac{\Delta\dot{\alpha}\bar{c}}{2\bar{V}} + \bar{C}_{l_{\delta_a}}\Delta\delta_a$$
$$+\bar{C}_{l_{\delta_e}}\Delta\delta_e + \bar{C}_{l_{\delta_r}}\Delta\delta_r + C_l\frac{\bar{h}dp_\infty}{p_\infty dh}\frac{\Delta h}{\bar{h}} \tag{13}$$

$$\frac{-\bar{I}_{xy}\dot{p}+\bar{I}_{yy}\dot{q}-\bar{I}_{yz}\dot{r}}{\bar{q}S\bar{c}} = \bar{C}_{m_p}\frac{pb}{2\bar{V}} + \bar{C}_{m_q}\frac{q\bar{c}}{2\bar{V}} + \bar{C}_{m_r}\frac{rb}{2\bar{V}} + \left(C_{m_V}+2C_m\right)\frac{\Delta V}{\bar{V}} + \bar{C}_{m_\alpha}\Delta\alpha + \bar{C}_{m_\beta}\Delta\beta + \bar{C}_{m_{\dot{\alpha}}}\frac{\Delta\dot{\alpha}\bar{c}}{2\bar{V}} + \bar{C}_{m_{\delta_a}}\Delta\delta_a$$
$$+\bar{C}_{m_{\delta_e}}\Delta\delta_e + \bar{C}_{m_{\delta_r}}\Delta\delta_r + \left[\frac{\left(\bar{T}_L+\bar{T}_R\right)z_e}{\bar{q}S\bar{c}} + C_m\right]\frac{\bar{h}dp_\infty}{p_\infty dh}\frac{\Delta h}{\bar{h}} + \left(\frac{\partial\bar{T}_L}{\partial V}+\frac{\partial\bar{T}_R}{\partial V}\right)\frac{z_e\bar{V}}{\bar{q}S\bar{c}}\frac{\Delta V}{\bar{V}} + \frac{\left(\Delta T_L+\Delta T_R\right)z_e}{\bar{q}S\bar{c}} \tag{14}$$

$$\frac{-\bar{I}_{xz}\dot{p}-\bar{I}_{yz}\dot{q}+\bar{I}_{zz}\dot{r}}{\bar{q}Sb} = \bar{C}_{n_p}\frac{pb}{2\bar{V}} + \bar{C}_{n_q}\frac{q\bar{c}}{2\bar{V}} + \bar{C}_{n_r}\frac{rb}{2\bar{V}} + \left(C_{n_V}+2C_n\right)\frac{\Delta V}{\bar{V}} + \bar{C}_{n_\alpha}\Delta\alpha + \bar{C}_{n_\beta}\Delta\beta + \bar{C}_{n_{\dot{\alpha}}}\frac{\Delta\dot{\alpha}\bar{c}}{2\bar{V}} + \bar{C}_{n_{\delta_a}}\Delta\delta_a$$
$$+\bar{C}_{n_{\delta_e}}\Delta\delta_e + \bar{C}_{n_{\delta_r}}\Delta\delta_r + \left[\frac{\left(\bar{T}_L-\bar{T}_R\right)y_e}{\bar{q}Sb} + C_n\right]\frac{\bar{h}dp_\infty}{p_\infty dh}\frac{\Delta h}{\bar{h}} + \left(\frac{\partial\bar{T}_L}{\partial V}-\frac{\partial\bar{T}_R}{\partial V}\right)\frac{y_e\bar{V}}{\bar{q}Sb}\frac{\Delta V}{\bar{V}} + \frac{\left(\Delta T_L-\Delta T_R\right)y_e}{\bar{q}Sb} \tag{15}$$

$$\frac{m\bar{V}}{\bar{q}S}\frac{\Delta\dot{V}}{\bar{V}} = \left[\frac{\bar{V}}{\bar{q}S}\left(\frac{\partial\bar{T}_L}{\partial V}+\frac{\partial\bar{T}_R}{\partial V}\right) - C_{D_V} + \bar{\beta}C_{Y_V} - 2C_D + 2\bar{\beta}C_Y\right]\frac{\Delta V}{\bar{V}} - \left[\frac{\bar{\alpha}\left(\bar{T}_L+\bar{T}_R\right)}{\bar{q}S} + C_{D_\alpha} - \bar{\beta}C_{Y_\alpha}\right]\Delta\alpha$$
$$-\left[\frac{\bar{\beta}\left(\bar{T}_L+\bar{T}_R\right)}{\bar{q}S} + C_{D_\beta} - \bar{\beta}C_D - \bar{\beta}C_{Y_\beta} + C_Y\right]\Delta\beta - \left(C_{D_{\dot{\alpha}}} - \bar{\beta}C_{Y_{\dot{\alpha}}}\right)\frac{\Delta\dot{\alpha}\bar{c}}{2\bar{V}} - \left(C_{D_p} - \bar{\beta}C_{Y_p}\right)\frac{pb}{2\bar{V}}$$
$$-\left(C_{D_q} - \bar{\beta}C_{Y_q}\right)\frac{q\bar{c}}{2\bar{V}} - \left(C_{D_r} - \bar{\beta}C_{Y_r}\right)\frac{rb}{2\bar{V}} - \left(C_{D_{\delta_a}} - \bar{\beta}C_{Y_{\delta_a}}\right)\Delta\delta_a - \left(C_{D_{\delta_e}} - \bar{\beta}C_{Y_{\delta_e}}\right)\Delta\delta_e - \left(C_{D_{\delta_r}} - \bar{\beta}C_{Y_{\delta_r}}\right)\Delta\delta_r$$
$$+\left(\frac{\bar{T}_L+\bar{T}_R}{\bar{q}S} - C_D + \bar{\beta}C_Y\right)\frac{\bar{h}dp_\infty}{p_\infty dh}\frac{\Delta h}{\bar{h}} + \frac{m\left(\dot{r}\Delta y-\dot{q}\Delta z\right) - m\bar{\beta}\left(\dot{r}\Delta x-\dot{p}\Delta z\right) + m\bar{\alpha}\left(\dot{q}\Delta x-\dot{p}\Delta y\right)}{\bar{q}S}$$
$$-\frac{mg\left(\Delta\theta-\bar{\phi}\Delta\beta-\Delta\alpha\right)}{\bar{q}S} + \frac{\left(\Delta T_L+\Delta T_R\right)}{\bar{q}S} \tag{16}$$

$$
\begin{aligned}
\frac{m\bar{V}\Delta\dot{\alpha}}{\bar{q}S} = &-\left[\frac{\bar{\alpha}\bar{V}}{\bar{q}S}\left(\frac{\partial\bar{T}_L}{\partial V}+\frac{\partial\bar{T}_R}{\partial V}\right)-\frac{\bar{\alpha}\left(T_L+T_R\right)}{\bar{q}S}+C_{L_V}+C_L\right]\frac{\Delta V}{\bar{V}}-\left(\frac{\bar{T}_L+\bar{T}_R}{\bar{q}S}+C_{L_\alpha}\right)\Delta\alpha \\
&-\left(\bar{\beta}C_L+C_{L_\beta}\right)\Delta\beta-C_{L_{\dot{\alpha}}}\frac{\Delta\dot{\alpha}\bar{c}}{2\bar{V}}-C_{L_p}\frac{pb}{2\bar{V}}-C_{L_q}\frac{q\bar{c}}{2\bar{V}}-C_{L_r}\frac{rb}{2\bar{V}}-C_{L_{\delta_a}}\Delta\delta_a-C_{L_{\delta_e}}\Delta\delta_e-C_{L_{\delta_r}}\Delta\delta_r \\
&-\left[\frac{\bar{\alpha}\left(\bar{T}_L+\bar{T}_R\right)}{\bar{q}S}+C_L\right]\frac{\bar{h}dp_\infty}{p_\infty dh}\frac{\Delta h}{\bar{h}}+\frac{m\bar{V}\left(q-\bar{\beta}p\right)}{\bar{q}S}+\frac{m\left(\dot{q}\Delta x-\dot{p}\Delta y\right)-m\bar{\alpha}\left(\dot{r}\Delta y-\dot{q}\Delta z\right)}{\bar{q}S} \\
&+\frac{mg\left(\bar{\gamma}\Delta\alpha-\bar{\gamma}\Delta\theta-\bar{\phi}\Delta\phi-\bar{\beta}\Delta\beta\right)}{\bar{q}S}-\frac{\left(\Delta T_L+\Delta T_R\right)\bar{\alpha}}{\bar{q}S}
\end{aligned}
\tag{17}
$$

$$
\begin{aligned}
\frac{m\bar{V}\Delta\dot{\beta}}{\bar{q}S} = &-\left[\frac{\bar{\beta}}{\bar{q}S}\left(\frac{\partial\bar{T}_L}{\partial V}+\frac{\partial\bar{T}_R}{\partial V}\right)-\frac{\bar{\beta}\left(\bar{T}_L+\bar{T}_R\right)}{\bar{q}S}-\bar{\beta}\left(C_{D_V}+C_D\right)-C_{Y_V}-C_Y\right]\frac{\Delta V}{\bar{V}}+\left(\bar{\beta}C_{D_\alpha}+C_{Y_\alpha}\right)\Delta\alpha \\
&-\left(\frac{\bar{T}_L+\bar{T}_R}{\bar{q}S}-C_D-\bar{\beta}C_{D_\beta}+\bar{\beta}C_Y-C_{Y_\beta}\right)\Delta\beta+\left(\bar{\beta}C_{D_{\dot{\alpha}}}+C_{Y_{\dot{\alpha}}}\right)\frac{\Delta\dot{\alpha}\bar{c}}{2\bar{V}}+\left(\bar{\beta}C_{D_p}+C_{Y_p}\right)\frac{pb}{2\bar{V}} \\
&+\left(\bar{\beta}C_{D_q}+C_{Y_q}\right)\frac{q\bar{c}}{2\bar{V}}+\left(\bar{\beta}C_{D_r}+C_{Y_r}\right)\frac{rb}{2\bar{V}}+\left(\bar{\beta}C_{D_{\delta_a}}+C_{Y_{\delta_a}}\right)\Delta\delta_a+\left(\bar{\beta}C_{D_{\delta_e}}+C_{Y_{\delta_e}}\right)\Delta\delta_e \\
&+\left(\bar{\beta}C_{D_{\delta_r}}+C_{Y_{\delta_r}}\right)\Delta\delta_r-\left[\frac{\bar{\beta}\left(\bar{T}_L+\bar{T}_R\right)}{\bar{q}S}-\bar{\beta}C_D-C_Y\right]\frac{\bar{h}dp_\infty}{p_\infty dh}\frac{\Delta h}{\bar{h}}-\frac{m\bar{V}\left(r-\bar{\alpha}p\right)}{\bar{q}S} \\
&-\frac{m\left(\dot{r}\Delta x-\dot{p}\Delta z\right)+\bar{\beta}\left(\dot{r}\Delta y-\dot{q}\Delta z\right)}{\bar{q}S}+\frac{mg\left(\bar{\gamma}\Delta\beta+\bar{\beta}\Delta\theta+\Delta\phi-\bar{\beta}\Delta\alpha\right)}{\bar{q}S}-\frac{\left(\Delta T_L+\Delta T_R\right)\bar{\beta}}{\bar{q}S}
\end{aligned}
\tag{18}
$$

$$\Delta\dot{\phi} = p+\bar{\theta}r \tag{19}$$

$$\Delta\dot{\theta} = q-\bar{\phi}r \tag{20}$$

$$\frac{\bar{h}}{\bar{V}}\frac{\Delta\dot{h}}{\bar{h}} = \bar{\gamma}\frac{\Delta V}{\bar{V}}+\Delta\theta-\Delta\alpha \tag{21}$$

In the equations above, the overbar symbol denotes a trim value. Also, the engine thrust is assumed to be a function of airspeed and vary linearly with the atmospheric pressure which is a function of altitude.[4] According to the 1976 U.S. Standard Atmosphere as,[4] the atmospheric pressure-altitude gradient can be evaluated to be

$$
\frac{\bar{h}dp_\infty}{p_\infty dh} = \begin{cases} \frac{-5.2561\left(6.875\times10^{-6}\bar{h}\right)}{1-6.875\times10^{-6}\bar{h}} & 0\le h\le 36089 \\ -4.806\times10^{-5}\bar{h} & 36089 < h \le 65617 \\ \frac{-34.164\left(1.0577\times10^{-6}\bar{h}\right)}{0.75189+1.0577\times10^{-6}(h-65617)} & 65617 < h \le 104990 \end{cases}
\tag{22}
$$

where $\bar{h}$ is the altitude at trim in feet.

Hence, the linearized equations of motion can be described by 9 states p,q, r, $\Delta V/\bar{V}$, $\Delta\alpha$, $\Delta\beta$, $\Delta\phi$, $\Delta\theta$, and $\Delta h/\bar{h}$. The control vector is comprised of $\Delta\delta_a$, $\Delta\delta_e$, $\Delta\delta_r$, ΔT_L, and ΔT_R. In the case of a vertical stabilizer separation damage, the rudder control is lost, hence $\Delta\delta_r = 0$.

A generic transport model (GTM) representative of a typical twin-engine transport aircraft is used for the study.[5] The aircraft has a nominal weight of 200,000 lbs and a weight of 197,772 lbs with no vertical stabilizer. The nominal inertia values are given by $I_{xx} = 1,770,000$ slug/ft^2, $I_{yy} = 5,680,000$ slug/ft^2, $I_{zz} = 7,270,000$ slug/ft^2, and $I_{xz} = 160,000$ slug/ft^2. With no vertical stabilizer, these inertia values are reduced to $I_{xx} = 1,740,105$ slug/ft^2, $I_{yy} = 5,306,737$ slug/ft^2, $I_{zz} = 6,926,598$ slug/ft^2, and $I_{xz} = 61,629$ slug/ft^2. The trim states and controls of the nominal GTM with symmetric thrusts and $\bar{\beta} = 0$ for three representative flight conditions at mach 0.4 and 10,000 ft; mach 0.6 and 20,000 ft; and mach 0.8 at 30,000 ft are presented in Table 1.

	Mach 0.4, 10K ft	Mach 0.6, 20K ft	Mach 0.8, 30K ft
$\bar{T}_L+\bar{T}_R$ (lb)	13,908	6,445	5,548
$\bar{\alpha}$ (deg)	7.180	4.230	2.899
$\bar{\phi}$ (deg)	0.001203	0.001668	0.002505
$\bar{\delta}_a$ (deg)	0.02866	0.02111	0.02212
$\bar{\delta}_e$ (deg)	−7.735	−5.994	−5.425
$\bar{\delta}_r$(deg)	−0.005026	−0.003971	−0.003965

Table 1 - Trim States and Controls for Nominal GTM

The open-loop poles of the aircraft for various degrees of separation damage to the vertical stabilizer for the selected flight conditions are shown in Tables 2 to 7.

	Mach 0.4, 10K ft	Mach 0.6, 20K ft	Mach 0.8, 30K ft
Short Period	$-0.6307 \pm j1.0469$	$-0.7099 \pm j1.3739$	$-0.7190 \pm j1.6226$
Phugoid	$-0.0010 \pm j0.0670$	$0.0001 \pm j0.0502$	$-0.0007 \pm j0.0250$
Roll	-1.2305	-1.5327	-1.6338
Spiral	-0.0411	-0.02550	-0.0177
Dutch-Roll	$-0.3939 \pm j1.3947$	$-0.3652 \pm j1.6026$	$-0.3207 \pm j1.7405$

Table 2 - Open-Loop Poles of Nominal GTM

	Mach 0.4, 10K ft	Mach 0.6, 20K ft	Mach 0.8, 20K ft
Short Period	$-0.6617 \pm j1.0380$	$-0.7451 \pm j1.3678$	$-0.7540 \pm j1.6211$
Phugoid	$-0.0008 \pm j0.0641$	$0.0000 \pm j0.04804$	$-0.0011 \pm j0.0214$
Roll	-1.2266	-1.5378	-1.6429
Spiral	-0.0473	-0.0305	-0.0214
Dutch-Roll	$-0.3443 \pm j1.2164$	$-0.3038 \pm j1.3574$	$-0.2568 \pm j1.4528$

Table 3 - Open-Loop Poles of Damaged GTM for 25% Break of Vertical Stabilizer

	Mach 0.4, 10K ft	Mach 0.6, 20K ft	Mach 0.8, 30K ft
Short Period	$-0.6704 \pm j1.0489$	$-0.7545 \pm j1.3818$	$-0.7633 \pm j1.6377$
Phugoid	$-0.0005 \pm j0.0600$	$0.0001 \pm j0.0450$	$-0.0019 \pm j0.0166$
Roll	-1.2084	-1.5423	-1.6569
Spiral	-0.0631	-0.0463	-0.0341
Dutch-Roll	$-0.2825 \pm j0.9268$	$-0.2222 \pm j0.9518$	$-0.1730 \pm j0.9840$

Table 4 - Open-Loop Poles of Damaged GTM for 57% Break of Vertical Stabilizer

	Mach 0.4, 10K ft	Mach 0.6, 20K ft	Mach 0.8, 30K ft
Short Period	$-0.6776 \pm j1.0606$	$-0.7623 \pm j1.3961$	$-0.7708 \pm j1.6538$
Phugoid	$-0.0003 \pm j0.0576$	$0.0001 \pm j0.0441$	$-0.0016 \pm j0.0183$
Roll	-1.1772	-1.5348	-1.6585
Spiral	-0.0919	-0.0874	-0.0713
Dutch-Roll	$-0.2536 \pm j0.7108$	$-0.1718 \pm j0.6317$	$-0.1218 \pm j0.6182$

Table 5 - Open-Loop Poles of Damaged GTM for 75% Break of Vertical Stabilizer

	Mach 0.4, 10K ft	Mach 0.6, 20K ft	Mach 0.8, 30K ft
Short Period	$-0.6812 \pm j1.0482$	$-0.7659 \pm j1.3802$	$-0.7742 \pm j1.6359$
Phugoid	$-0.0002 \pm j0.0541$	$0.0001 \pm j0.0414$	$-0.0034 \pm j0.0123$
Roll	-1.1235	-1.5211	-1.6578
Spiral	-0.2418	-0.5066	-0.5215
Dutch-Roll	$-0.1797 \pm j0.4097$	$0.0590 \pm j0.2480$	$0.1290 \pm j0.1741$

Table 6 - Open-Loop Poles of Damaged GTM for 88% Break of Vertical Stabilizer

	Mach 0.4, 10K ft	Mach 0.6, 20K ft	Mach 0.8, 30K ft
Short Period	$-0.6866 \pm j1.0658$	$-0.7719 \pm j1.4026$	$-0.7802 \pm j1.6619$
Phugoid	$-0.0001 \pm j0.0523$	$0.0001 \pm j0.0402$	-0.0037 ± 0.0114
Roll	-1.0855	-1.5121	-1.6557
Spiral	-0.4886	-0.6868	0.0853
Dutch-Roll	$-0.0626 \pm j0.2994$	$0.1584 \pm j0.1366$	$-0.6977, 0.3727$

Table 7 - Open-Loop Poles of Damaged GTM for 100% Break of Vertical Stabilizer

The resulting open-loop poles indicate that as airspeed and altitude increase, the open-loop yaw damping worsens and eventually becomes negative. It is interesting to note that at Mach 0.4 and 10,000 ft, the dutch-roll mode is still stable, though barely for a complete separation of the vertical stabilizer. This slight positive yaw damping is likely due to the dihedral effect.

III. Engine Dynamics

A typical engine response can be characterized by a time delay and time constant. The engine response time is generally due to the effects of fluid transport lag and the inertia of the mechanical systems such as rotors and turbomachinery blades. Engine dynamics are generally a highly complex, nonlinear process. A simplified engine dynamic model has been developed by NASA Glenn Research Center for use in this study.[6] The model is for a generic engine class and is based on actual flight test data collected at various flight conditions. The model generates the engine thrust response as a function of the throttle resolver angle (TRA) at a given flight condition specified by mach number and altitude.

Even with simplification, the complexity of the nonlinear model still makes it difficult for a flight control study. Thus, for this study, the nonlinear model is further simplified as a time-delayed second-order model as

$$\ddot{T} + 2\zeta\omega\dot{T} + \omega^2 T = \omega^2 T_c\,(t - t_d) \tag{23}$$

where ζ and ω are the damping ratio and bandwidth frequency of the closed-loop engine dynamics, and T_c is the engine thrust command which is prescribed by an engine TRA.

The engine time delay t_d is generally dependent on the initial thrust level according to an inverse relationship. That is, the larger the initial thrust level that an engine operates at, the smaller the engine time delay is. The time constant of the engine response dictates how fast the engine thrust rises. The time constant may be defined as

$$\tau = \frac{1}{\omega} \tag{24}$$

The damping ratio for the closed-loop engine dynamics can be selected as $\zeta = 1$ which represents a critically-damped engine response. Then, the engine model can be written as

$$\begin{bmatrix} \dot{T} \\ \ddot{T} \end{bmatrix} = \begin{bmatrix} 0 & 1 \\ -\frac{1}{\tau^2} & -\frac{2}{\tau} \end{bmatrix} \begin{bmatrix} T \\ \dot{T} \end{bmatrix} + \begin{bmatrix} 0 \\ \frac{1}{\tau^2} \end{bmatrix} T_c\,(t - t_d) \tag{25}$$

The engine response curves are shown in Figs. 1, 2, and 3 for the three representative flight conditions at mach 0.4 at 10,000 ft; mach 0.6 and 20,000 ft; and mach 0.8 and 30,000 ft. The time-delay second-order system approximates the engine thrust response reasonably well for mach 0.4 and mach 0.6 flight conditions. At mach 0.8, the approximate model still trends well, although the time delay response is slightly on the conservative side. In general, it can be seen that the engine time delay and time constant increase with mach number and altitude. This is due to the reduced trim thrust of the engines.

It should be noted that the engine dynamics for a thrust increase and a thrust decrease are not the same. In general, it is observed that engine dynamics are somewhat faster in the response time when a thrust reduction is commanded.

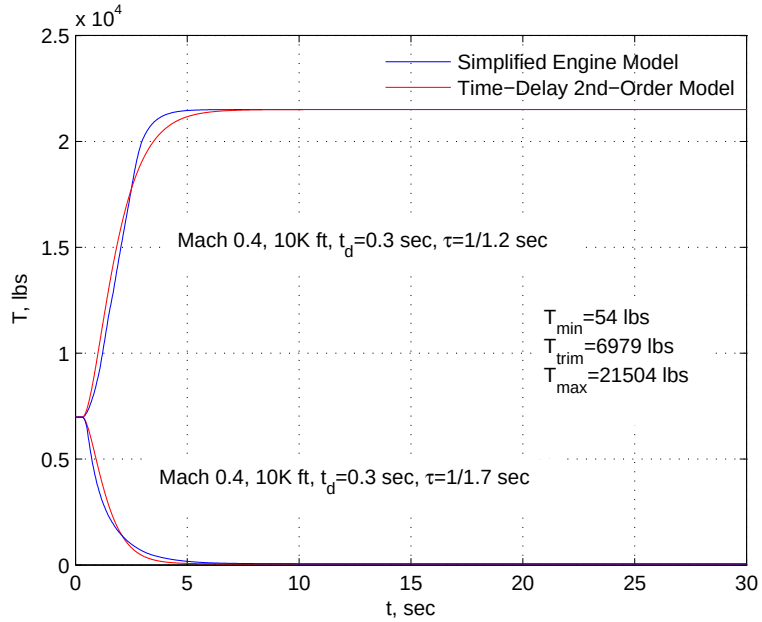

Fig. 1 - Engine Thrust Response at Mach 0.4 and 10,000 ft

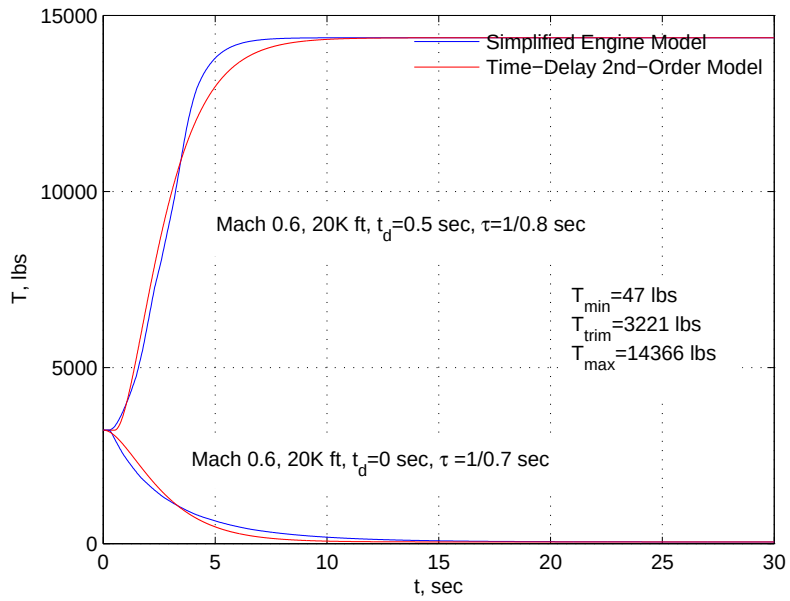

Fig. 2 - Engine Thrust Response at Mach 0.6 and 20,000 ft

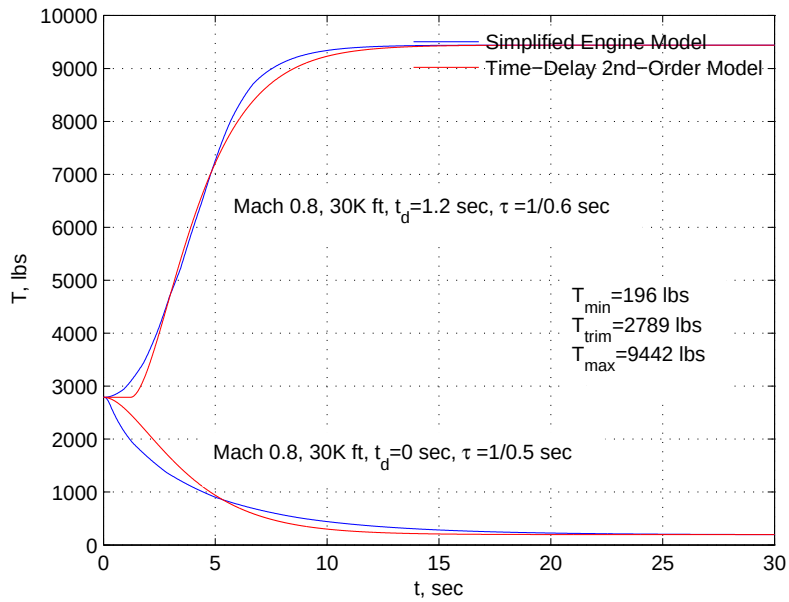

Fig. 3 - Engine Thrust Response at Mach 0.8 and 30,000 ft

IV. Engine Response Requirements for Flight Propulsion Control

For the nominal aircraft, the yaw damper can be designed to improve the dutch-roll mode. The lateral-directional linear equations with the aileron and rudder controls are given by

$$\begin{bmatrix} \Delta\dot{\phi} \\ \dot{p} \\ \Delta\dot{\beta} \\ \dot{r} \end{bmatrix} = \begin{bmatrix} 0 & 1 & 0 & \bar{\theta} \\ 0 & L_p & L_\beta & L_r \\ \frac{g}{\bar{V}} & \frac{Y_p}{\bar{V}} & \frac{Y_\beta + g\bar{\gamma}}{\bar{V}} & \frac{Y_r}{\bar{V}} - 1 \\ 0 & N_p & N_\beta & N_r \end{bmatrix} \begin{bmatrix} \Delta\phi \\ p \\ \Delta\beta \\ r \end{bmatrix} + \begin{bmatrix} 0 & 0 \\ L_{\delta_a} & L_{\delta_r} \\ \frac{Y_{\delta_a}}{\bar{V}} & \frac{Y_{\delta_r}}{\bar{V}} \\ N_{\delta_a} & N_{\delta_r} \end{bmatrix} \begin{bmatrix} \Delta\delta_a \\ \Delta\delta_r \end{bmatrix} \tag{26}$$

Let the desired dutch-roll damping ratio and frequency be $\zeta = 0.5$. Choosing a simple yaw rate feedback control $\Delta\delta_r = k_r^* r$ and neglecting the implementation of a wash-out filter in a classical yaw damper,[7] then the feedback yaw damper can be designed to give the closed-loop system the desired dutch-roll eigenvalues of . The results are shown in Table 8

	Mach 0.4, 10K ft	Mach 0.6, 20K ft	Mach 0.8, 30K ft
k_r^*	0.7497	0.5869	0.5530
Roll	-1.2626	-1.5503	-1.6484
Spiral	-0.1675	-0.1118	-0.0925
Dutch-Roll	$-0.7384 \pm j1.2789$	$-0.8375 \pm j1.4506$	$-0.8971 \pm j1.5538$
ζ	0.5	0.5	0.5
ω_n, rad/sec	1.4768	1.6750	1.7942

Table 8 - Closed-Loop Poles of Nominal GTM Using Rudder Yaw Rate Feedback

Now suppose that the rudder system is disabled and the engines are used as alternate control effectors, the lateral-directional linear equations with the aileron and engine controls are given by

$$\begin{bmatrix} \Delta\dot{\phi} \\ \dot{p} \\ \Delta\dot{\beta} \\ \dot{r} \end{bmatrix} = \begin{bmatrix} 0 & 1 & 0 & \bar{\theta} \\ 0 & L_p & L_\beta & L_r \\ \frac{g}{\bar{V}} & \frac{Y_p}{\bar{V}} & \frac{Y_\beta + g\bar{\gamma}}{\bar{V}} & \frac{Y_r}{\bar{V}} - 1 \\ 0 & N_p & N_\beta & N_r \end{bmatrix} \begin{bmatrix} \Delta\phi \\ p \\ \Delta\beta \\ r \end{bmatrix} + \begin{bmatrix} 0 & 0 & 0 \\ L_{\delta_a} & \frac{\bar{I}_{xz} y_e}{\bar{I}_{xx}\bar{I}_{zz} - \bar{I}_{xz}^2} & 0 \\ \frac{Y_{\delta_a}}{\bar{V}} & 0 & -\frac{\bar{\beta}}{m\bar{V}} \\ N_{\delta_a} & \frac{\bar{I}_{xx} y_e}{\bar{I}_{xx}\bar{I}_{zz} - \bar{I}_{xz}^2} & 0 \end{bmatrix} \begin{bmatrix} \Delta\delta_a \\ \Delta\delta T \\ \Delta T \end{bmatrix} \tag{27}$$

where $\Delta\delta T = \Delta T_L - \Delta T_R$ is the differential engine thrust (left engine thrust minus right engine thrust) and $\Delta T = \Delta T_L + \Delta T_R$ is the collective engine thrust (left engine thrust plus right engine thrust).

If the initial trim sideslip angle is zero, then ΔT has no contribution to the control effectiveness for a small perturbation about the trim point. Then, the control variables are the aileron $\Delta\delta_a$ and the engine differential thrust $\Delta\delta T$ which replaces the rudder control $\Delta\delta_r$. The goal is for the engines to provide a directional stability augmentation as a yaw damper. Choosing a simple yaw rate feedback $\Delta\delta T = k_r r$ and neglecting the engine dynamics and engine thrust limits which will be considered later, then the propulsion control yaw damper can be designed to give the closed-loop system the desired dutch-roll damping ratio.

Consider first a nominal aircraft with a disabled rudder system, the results of the propulsion control yaw damper are shown in Table 9

	Mach 0.4, 10K ft	Mach 0.6, 20K ft	Mach 0.8, 30K ft
k_r	$-152,411$	$-186,474$	$-218,780$
Roll	-1.2769	-1.5633	-1.6611
Spiral	-0.1894	-0.1348	-0.1162
Dutch-Roll	$-0.7481 \pm j1.2958$	$-0.8478 \pm j1.4684$	$-0.9061 \pm j1.5694$
ζ	0.5	0.5	0.5
ω_n, rad/sec	1.4962	1.6956	1.8122

Table 9 - Closed-Loop Poles of GTM with Disabled Rudder Using Differential Thrust Yaw Rate Feedback

All the lateral-directional modes are shown to be stable without considering the effects of the engine dynamics and engine thrust limits.

To reduce the demand of the engine thrust, the aileron can also be used for yaw damper. Let $x = \begin{bmatrix} \Delta\phi & p & \Delta\beta & r \end{bmatrix}^\top$ and $u = \begin{bmatrix} \Delta\delta_a & \Delta\delta T \end{bmatrix}^\top$, then the system can be written as

$$\dot{x} = Ax + Bu \tag{28}$$

The desired closed-loop dynamics of the nominal aircraft is

$$\dot{x} = (A^* + B^* K^*)\, x \tag{29}$$

where the asterisk denotes the matrices of the nominal aircraft with rudder yaw rate feedback yaw damper.

Then the aileron-differential thrust state feedback yaw damper can be computed using a pseudo-inverse control as $u = Kx$ where

$$K = \left(B^\top B\right)^{-1} B^\top \left(A^* + B^* K^* - A\right) \tag{30}$$

The computed state feedback gains are shown in Table 10.

	Mach 0.4, 10K ft	Mach 0.6, 20K ft	Mach 0.8, 30K ft
K	$\begin{bmatrix} 0 & 0 \\ 0 & 0 \\ 0 & 0 \\ 0.1586 & -142,076 \end{bmatrix}$	$\begin{bmatrix} 0 & 0 \\ 0 & 0 \\ 0 & 0 \\ 0.1674 & -177,088 \end{bmatrix}$	$\begin{bmatrix} 0 & 0 \\ 0 & 0 \\ 0 & 0 \\ 0.1694 & -210,618 \end{bmatrix}$
Roll	-1.2633	-1.5509	-1.6488
Spiral	-0.1633	-0.1091	-0.0904
Dutch-Roll	$-0.7402 \pm j1.2995$	$-0.8386 \pm j1.4731$	$-0.8980 \pm j1.5772$
ζ	0.4949	0.4947	0.4948
ω_n, rad/sec	1.4955	1.6951	1.8149

Table 10 - Closed-Loop Poles of GTM with Disabled Rudder using Aileron and Differential Thrust State Feedback

Now consider the worst-case scenario for an aircraft with a complete separation of the vertical stabilizer. Using only a yaw rate feedback propulsion control, it is not possible to stabilize the aircraft in the lateral-directional motion. Using the aileron as an additional control effector, the state feedback propulsion control is able to stabilize the aircraft. The computed state feedback gains are given in Table 11.

	Mach 0.4, 10K ft	Mach 0.6, 20K ft	Mach 0.8, 30K ft
$K^\top$	$\begin{bmatrix} 0 & 0 \\ -0.0044 & 7,297 \\ -0.2800 & 272,279 \\ 0.1875 & -178,600 \end{bmatrix}$	$\begin{bmatrix} 0 & 0 \\ -0.0061 & 7,818 \\ -0.4061 & 432,147 \\ 0.1977 & -215,106 \end{bmatrix}$	$\begin{bmatrix} 0 & 0 \\ -0.0053 & 7,362 \\ -0.4350 & 533,883 \\ 0.1932 & -244,952 \end{bmatrix}$
Roll	-1.2648	-1.5514	-1.6486
Spiral	-0.1689	-0.1128	-0.0933
Dutch-Roll	$-0.6991 \pm j1.2928$	$-0.7959 \pm j1.4648$	$-0.8577 \pm j1.5676$
ζ	0.4757	0.4774	0.4800
ω_n, rad/sec	1.4697	1.6671	1.7869

Table 11 - Closed-Loop Poles of GTM with 100% Break of Vertical Stabilizer using Aileron and Differential Thrust State Feedback

A. Flight-Propulsion Dynamics

Assuming that the aileron is a fast acting actuator, then the aileron actuator output follow the aileron command closely so that $\Delta\delta_a \approx \Delta\delta_{a,c}$. In the case of the differential engine thrust command, the effects of the slow engine lag and time constant must be taken into account. Toward this end, the perturbation of the differential engine dynamics can be expressed as

$$\begin{bmatrix} \Delta\delta\dot{T}(t) \\ \Delta\delta\ddot{T}(t) \end{bmatrix} = \begin{bmatrix} 0 & 1 \\ -\frac{1}{\tau^2} & -\frac{2}{\tau} \end{bmatrix} \begin{bmatrix} \Delta\delta T(t) \\ \Delta\delta\dot{T}(t) \end{bmatrix} + \begin{bmatrix} 0 \\ \frac{1}{\tau^2} \end{bmatrix} \Delta\delta T_c(t-t_d) \tag{31}$$

The differential engine thrust command is given by

$$\Delta\delta T_c = K_2 x \tag{32}$$

where $K = \begin{bmatrix} K_1^\top & K_2^\top \end{bmatrix}^\top$.

The flight-propulsion dynamics can be represented as an input-delay system as

$$\begin{bmatrix} \dot{x}(t) \\ \Delta\delta\dot{T}(t) \\ \Delta\delta\ddot{T}(t) \end{bmatrix} = \begin{bmatrix} A & B_2 & 0 \\ 0 & 0 & 1 \\ 0 & -\frac{1}{\tau^2} & -\frac{2}{\tau} \end{bmatrix} \begin{bmatrix} x(t) \\ \Delta\delta T(t) \\ \Delta\delta\dot{T}(t) \end{bmatrix} + \begin{bmatrix} B_1 & 0 \\ 0 & 0 \\ 0 & \frac{1}{\tau^2} \end{bmatrix} \begin{bmatrix} \Delta\delta_a(t) \\ \Delta\delta T_c(t-t_d) \end{bmatrix} \tag{33}$$

where $B = \begin{bmatrix} B_1 & B_2 \end{bmatrix}$.

Substituting (32) then yields the closed-loop flight-propulsion dynamics

$$\begin{bmatrix} \dot{x}(t) \\ \Delta\delta\dot{T}(t) \\ \Delta\delta\ddot{T}(t) \end{bmatrix} = \begin{bmatrix} A+B_1K_1 & B_2 & 0 \\ 0 & 0 & 1 \\ 0 & -\frac{1}{\tau^2} & -\frac{2}{\tau} \end{bmatrix} \begin{bmatrix} x(t) \\ \Delta\delta T(t) \\ \Delta\delta\dot{T}(t) \end{bmatrix} + \begin{bmatrix} 0 & 0 & 0 \\ 0 & 0 & 0 \\ \frac{1}{\tau^2}K_2 & 0 & 0 \end{bmatrix} \begin{bmatrix} x(t-t_d) \\ \Delta\delta T(t-t_d) \\ \Delta\delta\dot{T}(t-t_d) \end{bmatrix} \tag{34}$$

B. Engine Time Constant Requirement

Equation (34) can be written as

$$\dot{z}(t) = A_c(\tau)z(t) + A_t(\tau)z(t-t_d) \tag{35}$$

Consider the case when the engine lag is negligible so that $t_d \approx 0$, then the flight-propulsion closed-loop system is

$$\dot{z}(t) = (A_c(\tau) + A_t(\tau))z(t) \tag{36}$$

or

$$\begin{bmatrix} \dot{x}(t) \\ \Delta\delta\dot{T}(t) \\ \Delta\delta\ddot{T}(t) \end{bmatrix} = \begin{bmatrix} A+B_1K_1 & B_2 & 0 \\ 0 & 0 & 1 \\ \frac{1}{\tau^2}K_2 & -\frac{1}{\tau^2} & -\frac{2}{\tau} \end{bmatrix} \begin{bmatrix} x(t) \\ \Delta\delta T(t) \\ \Delta\delta\dot{T}(t) \end{bmatrix} \tag{37}$$

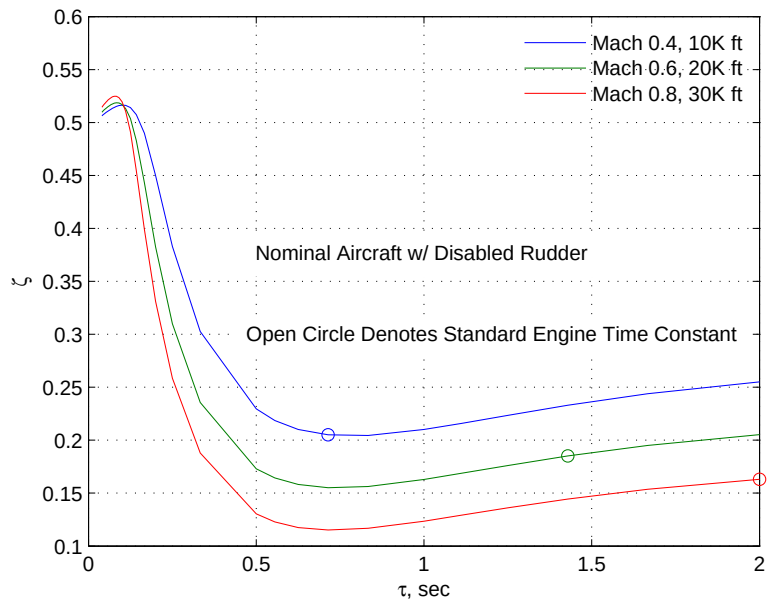

Fig. 4 - Dutch-Roll Damping of Nominal GTM with Disabled Rudder

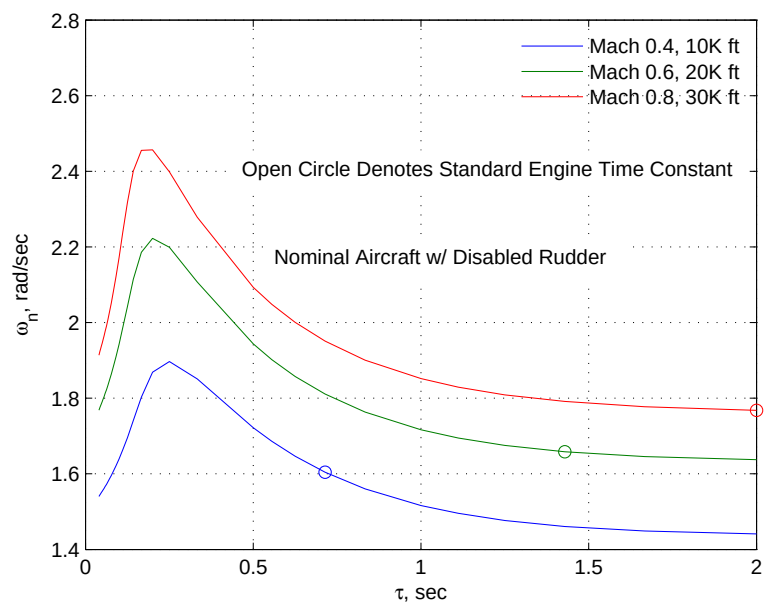

Fig. 5 - Dutch-Roll Frequency of Nominal GTM with Disabled Rudder

Figures 4 and 5 show the effects of the engine time constant on the dutch-roll damping ratio and frequency for the nominal GTM with a disabled rudder system. As can be seen, the dutch-roll damping ratio generally increases with decreasing the engine time constant. For a time constant of 0.4 or higher, the dutch-roll damping does not seem to change significantly. Even though a dutch-roll damping ratio of 0.5 is desired, a value as low as 0.3 also may be

acceptable for handling qualities. The engine time constant requirements for flight-propulsion control of the nominal GTM with a disabled rudder system are shown in Table 12. Comparing the results with the standard time constants from Figs. 1 to 3, the increase in the engine time constant ranges from 2 to 9 times for a dutch-roll damping ratio of 0.3 and from 5 to 17 times for a dutch-roll damping ratio of 0.5.

	Mach 0.4, 10K ft	Mach 0.6, 20K ft	Mach 0.8, 30K ft
τ, sec nominal	0.71	1.43	2.00
τ, sec for $\zeta = 0.3$	0.3394	0.2611	0.2215
τ, sec for $\zeta = 0.5$	0.1529	0.1281	0.1186

Table 12 - Engine Time Constant for Flight-Propulsion Control of GTM with Disabled Rudder

Figures 6 and 7 are plots of the dutch-roll damping ratio and frequency for a damaged GTM with 100% break of the vertical stabilizer as a function of the engine time constant. Because the damage is the most severe, the engine time constant requirements even for the damping ratio of 0.3, as shown in Table 13, can be quite demanding. The increase in the engine time constant ranges from 5 to 21 times. Because the demand is quite extreme at high speed and altitude, there is a practical limitation of how much flight-propulsion control can be used for directional stability augmentation. It is noted that for a typical bandwidth of 4 Hz for a rudder actuator, this corresponds to a time constant of 0.04 sec. So if the engine response is as fast as the rudder actuator, then a dutch-roll damping ratio of about 0.42 could be achieved using a flight-propulsion control strategy. This implies that effectively an engine should be as fast as a rudder system in theory in order to provide a similar level of handling qualities in the dutch-roll mode.

	Mach 0.4, 10K ft	Mach 0.6, 20K ft	Mach 0.8, 30K ft
τ, sec nominal	0.71	1.43	2.00
τ, sec for $\zeta = 0.3$	0.1332	0.1033	0.0939

Table 13 - Engine Time Constant for Flight-Propulsion Control of GTM with 100% Break of Vertical Stabilizer

The assumption of $t_d = 0$ in the above analysis is not realistic since the engine lag can be significant and can destabilize the closed-loop system. However, the time constant requirements for $t_d = 0$ provide an upper bound on the engine response requirements. With the presence of the engine lag, it is expected that the time constant requirements should be smaller than these estimates.

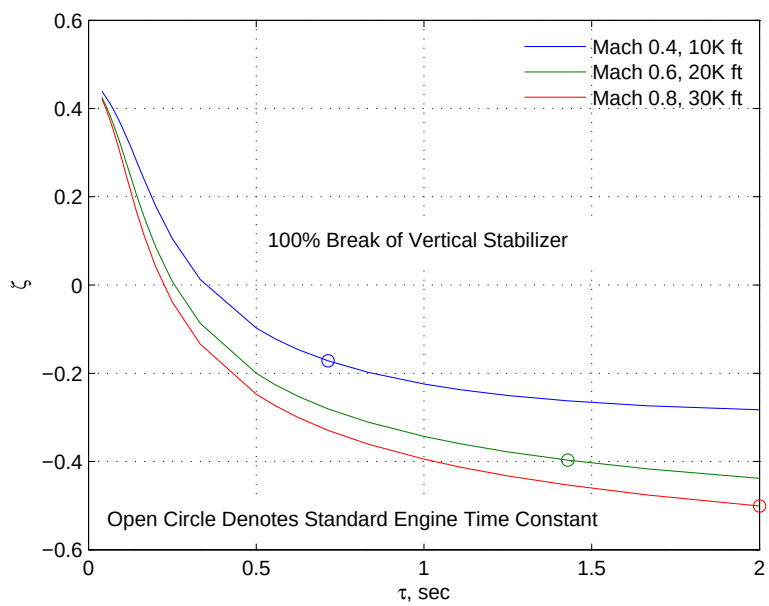

Fig. 6 - Dutch-Roll Damping of GTM with 100% Break of Vertical Stabilizer

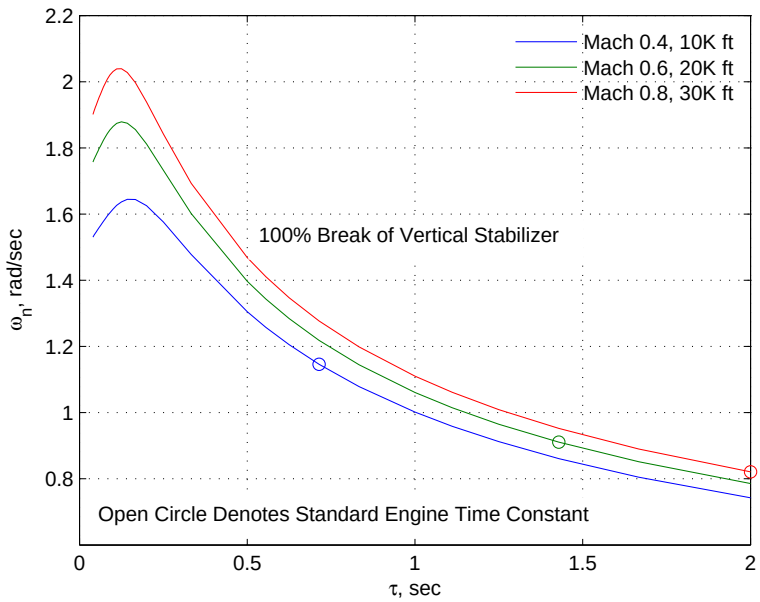

Fig. 7 - Dutch-Roll Frequency of GTM with 100% Break of Vertical Stabilizer

C. Engine Time Delay Requirements

The presence of the time delay in Eq. (34) poses some difficulty which stability analysis. Pade approximation can usually be used to approximate a time-delay system as a higher-order system. Alternatively, a first-order Euler's method can also be used by recognizing that

$$e^{-t_s s} = 1 - t_d s + \mathscr{O}\left(s^2\right) \tag{38}$$

The first-order Euler's method provides a reasonably conservative estimate of stability of a first-order system,[8] and is easier to implement than the Pade approximation which increases the order of the system.

Then, Eq. (34) can be expressed by the Laplace transform as

$$sz = A_c z + A_t e^{-t_s s} z \approx A_c z + A_t \left(1 - t_d s\right) z \tag{39}$$

or in the time domain as

$$\dot{z}(t) \approx \left(I + A_t t_d\right)^{-1} \left(A_c + A_t\right) z(t) \tag{40}$$

Figures 8 and 9 show the effect of the engine time delay due to the engine lag on the dutch-roll damping ratio and frequency for the nominal GTM with a disabled rudder system. The time constant of the engines is chosen such that the initial value is 0.5. As the engine lag increases, the aircraft becomes less stable directionally. With the standard engine lag, which is assumed to be 0.3 sec at mach 0.4 and 10,000 ft, 0.5 sec at mach 0.6 and 20,000 ft, and 0.7 sec at mach 0.8 and 30,000 ft (obtained by linear extrapolation since the time delay from the model is conservative), the damping ratio becomes worsened as the airspeed and altitude increase. At mach 0.8 and 30,000 ft, the aircraft is unstable. At mach 0.4 and 10,000 ft, there is still sufficient damping ratio that maintains directional stability of the aircraft. At mach 0.6 and 20,000 ft, the damping ratio is quite low that can result in poor handling qualities. To maintain a damping ratio of 0.3, the engine lag needs to be reduced. Table 14 shows the maximum engine time delay for the nominal GTM with a disabled rudder system at various flight conditions.

	Mach 0.4, 10K ft	Mach 0.6, 20K ft	Mach 0.8, 30K ft
t_d, sec nominal	0.3	0.4	0.5
t_d, sec for $\zeta = 0.3$	0.4117	0.3100	0.2411

Table 14 - Engine Time Delay for Flight-Propulsion Control of GTM with Disabled Rudder

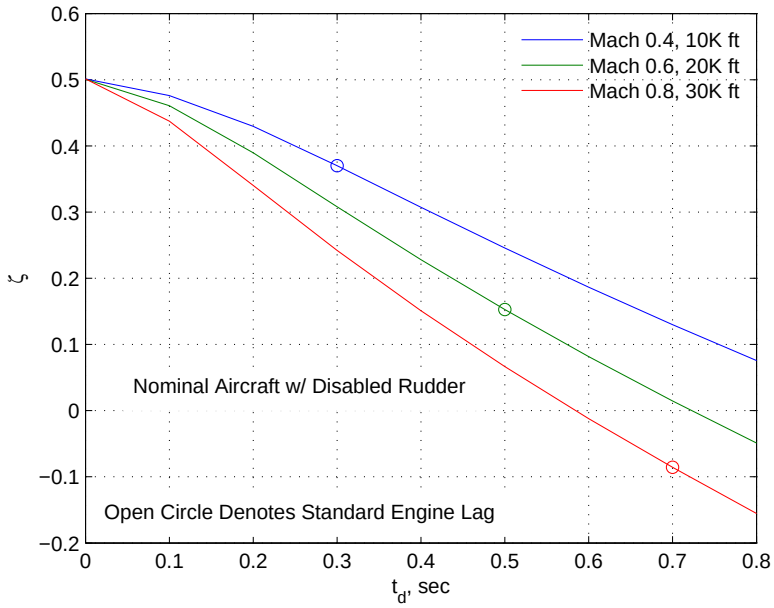

Fig. 8 - Dutch-Roll Damping of Nominal GTM with Disabled Rudder

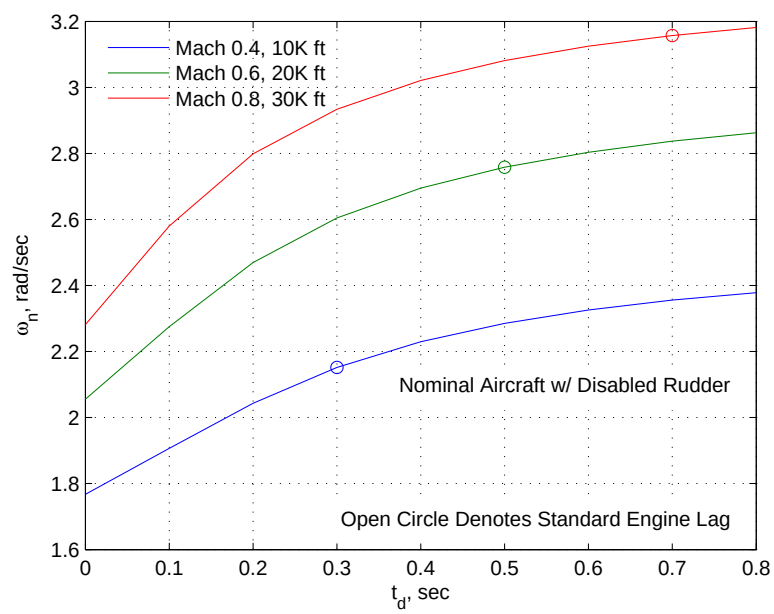

Fig. 9 - Dutch-Roll Frequency of Nominal GTM with Disabled Rudder

Figures 10 and 11 are plots of the dutch-roll damping ratio and frequency for a damaged GTM with 100% break of the vertical stabilizer as a function of the engine lag. The initial damping ratio is chosen such that the initial value is 0.4, which corresponds to an engine time constant of 0.0724 sec at mach 0.4 and 10,000 ft, 0.0556 sec at mach 0.6 and 20,000 ft, and 0.0518 sec at mach 0.8 and 30,000 ft. The aircraft is unstable at both mach 0.6 and mach 0.8 conditions. At mach 0.4 and 10,000 ft, the damping ratio is still positive, so the aircraft is still controllable directionally. This analysis suggests that flight-propulsion control is more effective at low airspeed and altitude than at high airspeed and altitude. Table 15 shows the maximum engine time delay for the nominal GTM with 100% break of the vertical stabilizer at various flight conditions.

	Mach 0.4, 10K ft	Mach 0.6, 20K ft	Mach 0.8, 30K ft
t_d, sec nominal	0.3	0.4	0.5
t_d, sec for $\zeta = 0.3$	0.1439	0.1119	0.1000

Table 15 - Engine Time Delay for Flight-Propulsion Control of GTM with 100% Break of Vertical Stabilizer

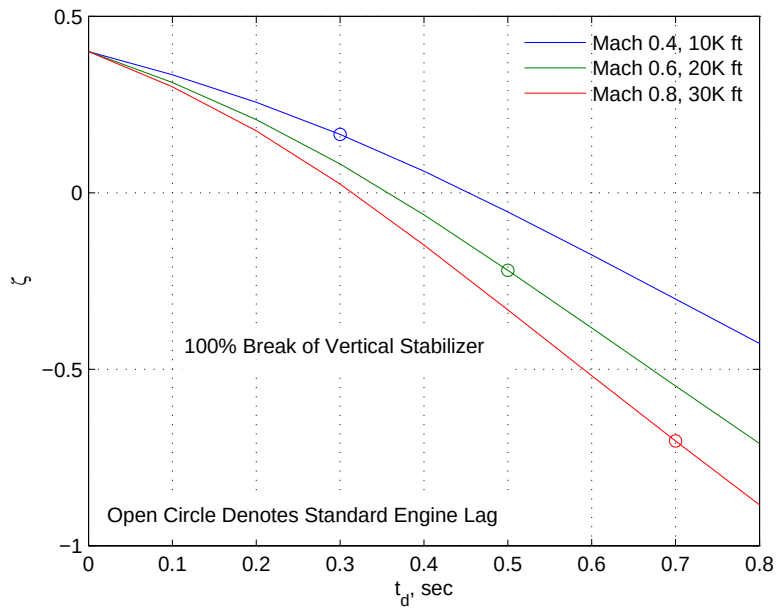

Fig. 10 - Dutch-Roll Damping of GTM with 100% Break of Vertical Stabilizer

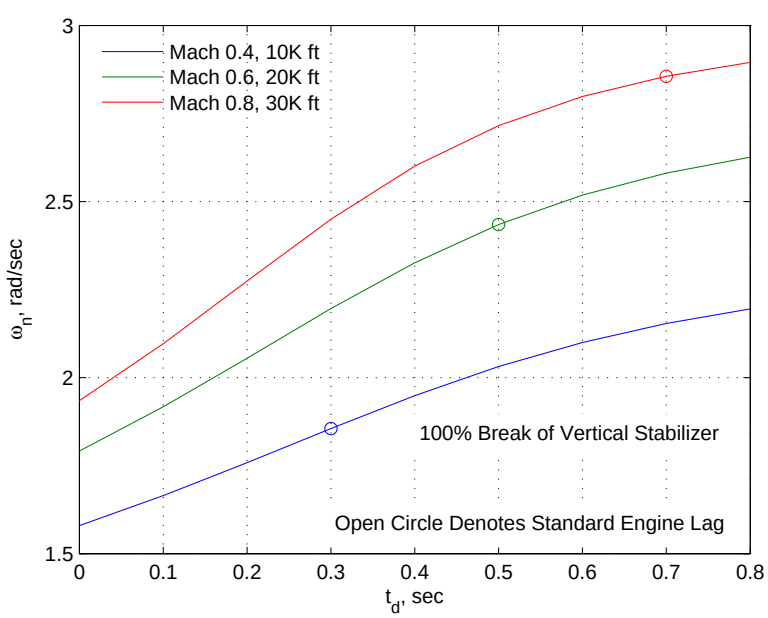

Fig. 11 - Dutch-Roll Frequency of GTM with 100% Break of Vertical Stabilizer

D. Effect of Engine Thrust Saturation

When the engine thrust reach its maximum or minimum limiting value, the effectiveness of flight-propulsion control is reduced. The control system is nonlinear due to the engine thrust saturation. Moreover, the collective thrust also

changes and causes the airspeed and angle of attack to change. Stability of a control saturation is difficult to analyze using linear analysis tools. Simulations can be performed to assess the effect of engine thrust saturation on the aircraft directional stability. It should also be noted that aircraft maneuverability also depends on the engine thrust, so that maintaining stability and maneuverability can compound the demand of aircraft engines for flight-propulsion control.

V. Simulations

Simulations of flight-propulsion control are conducted to verify the analysis. The simulation model is comprised of a linear aircraft model with a time-delay second-order linear engine model. The initial conditions are $\beta(0) = 5$ deg and $r(0) = 1$ deg. Figures 12 and 13 are the response of and the control inputs for the nominal GTM with a disabled rudder system at mach 0.8 and 30,000 ft with the nominal engine response corresponding to a dutch-roll damping ratio of 0.1707 for $\tau = 2$ sec and $t_d = 0.7$ sec. Figures 14 and 15 are the response of and the control inputs with a fast engine response where the time constant and time delay are reduced to $\tau = 0.1186$ sec and $t_d = 0.3$ sec, respectively. The response can be seen to improve. In any case, with a disabled rudder system, the aircraft is controllable using the differential engine thrust control.

Figures 16 and 17 are the response of and the control inputs for the GTM with 100% break of the vertical stabilizer at mach 0.8 and 30,000 ft with the nominal engine response corresponding to a negative dutch-roll damping ratio of -0.5629, which indicates an unstable aircraft. Figures 18 and 19 are the response and control inputs for a fast engine response with the time constant and time delay reduced to $\tau = 0.0518$ sec and $t_d = 0.3$ sec, respectively. The corresponding dutch-roll damping ratio is 0.024 which indicates a very lightly damped aircraft. The response is highly oscillatory and the yaw rate is not well damped. The engine thrusts are quite active in order to control the lightly damped dutch-roll mode. Realistically, an aircraft with no vertical stabilizer may not be controllable at this flight condition using flight-propulsion control since the engine response time may not be attainable due to the physical limitation of the engine performance. This damage scenario at this flight condition may represent the most challenge to flight-propulsion control. As the airspeed and altitude decrease, flight-propulsion control would become more effective.since the engine thrust capability generally increases with decreasing altitude.

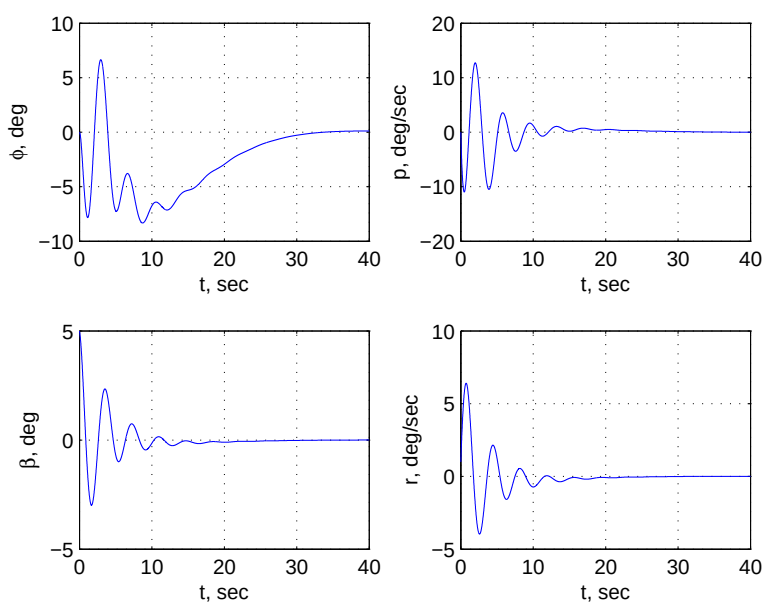

Fig. 12 - Response of GTM with Disabled Rudder at Mach 0.8 and 30K ft with Nominal Engine Response ($\zeta = 0.1707$, $\tau = 2$ sec, $t_d = 0.7$ sec)

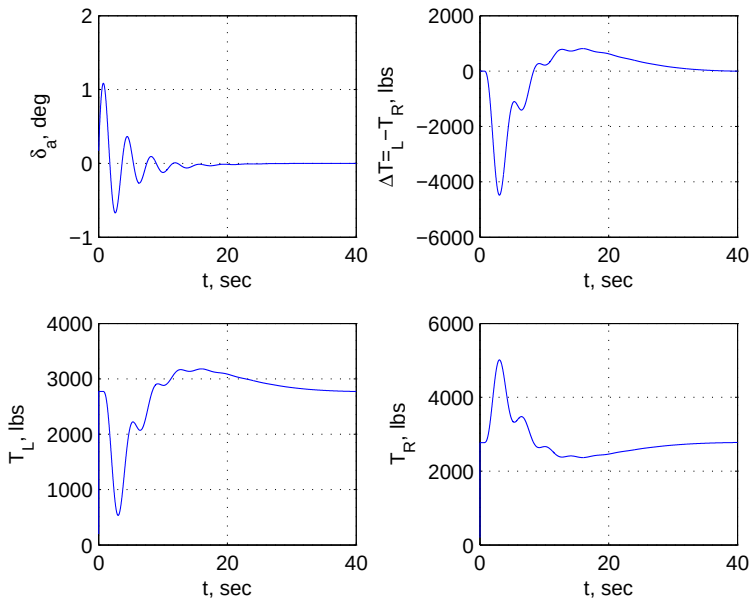

Fig. 13 - Aileron and Engine Thrusts for GTM with Disabled Rudder at Mach 0.8 and 30K ft with Nominal Engine Response ($\zeta = 0.1707$, $\tau = 2$ sec, $t_d = 0.7$ sec)

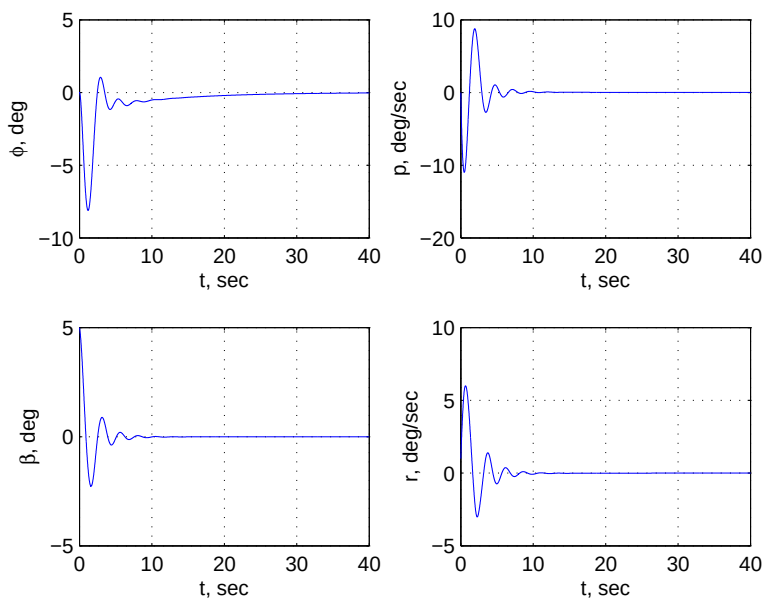

Fig. 14 - Response of GTM with Disabled Rudder at Mach 0.8 and 30K ft with Fast Engine Response ($\zeta = 0.2421$, $\tau = 0.1186$ sec, $t_d = 0.3$ sec)

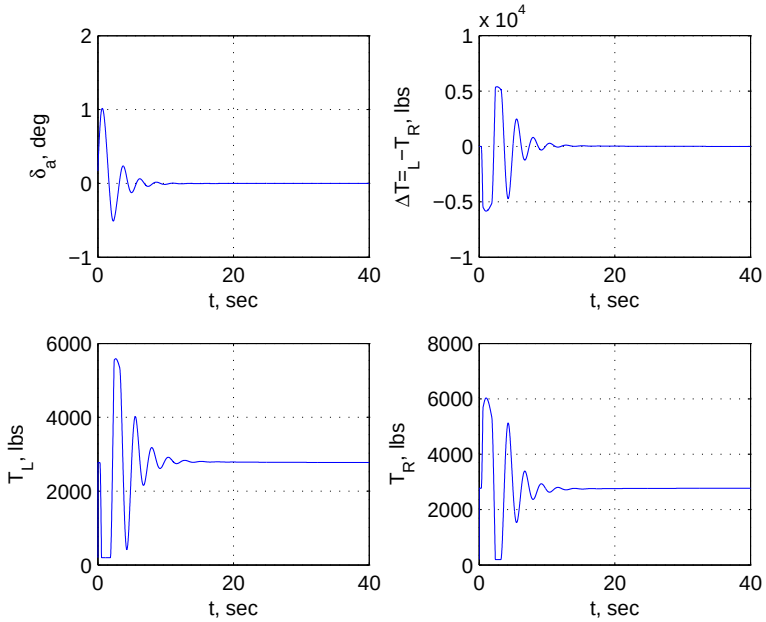

Fig. 15 - Aileron and Engine Thrusts for GTM with Disabled Rudder at Mach 0.8 and 30K ft with Fast Engine Response ($\zeta = 0.2421$, $\tau = 0.1186$ sec, $t_d = 0.3$ sec)

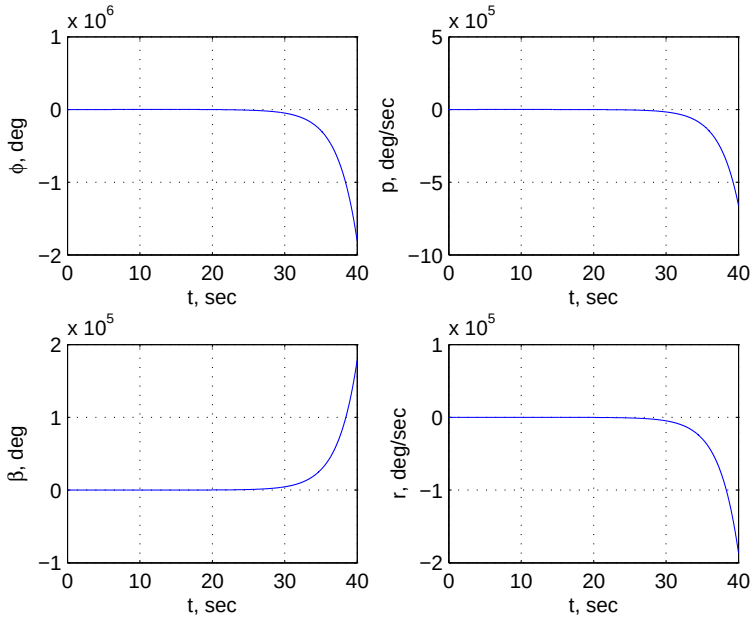

Fig. 16 - Response of GTM with 100% Break of Vertical Stabilizer at Mach 0.8 and 30K ft with Nominal Engine Response ($\zeta = -0.5629$, $\tau = 2$ sec, $t_d = 0.7$ sec)

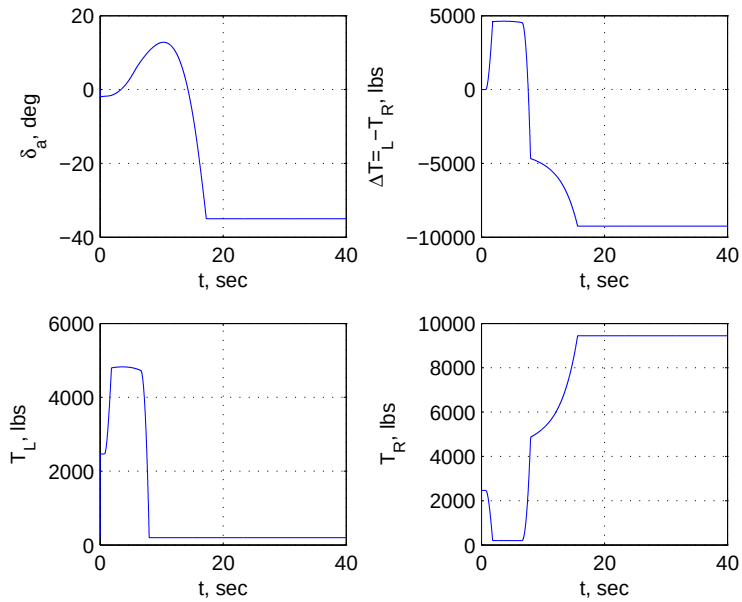

Fig. 17 - Aileron and Engine Thrusts for GTM with 100% Break of Vertical Stabilizer at Mach 0.8 and 30K ft with Nominal Engine Response ($\zeta = -0.5629$, $\tau = 2$ sec, $t_d = 0.7$ sec)

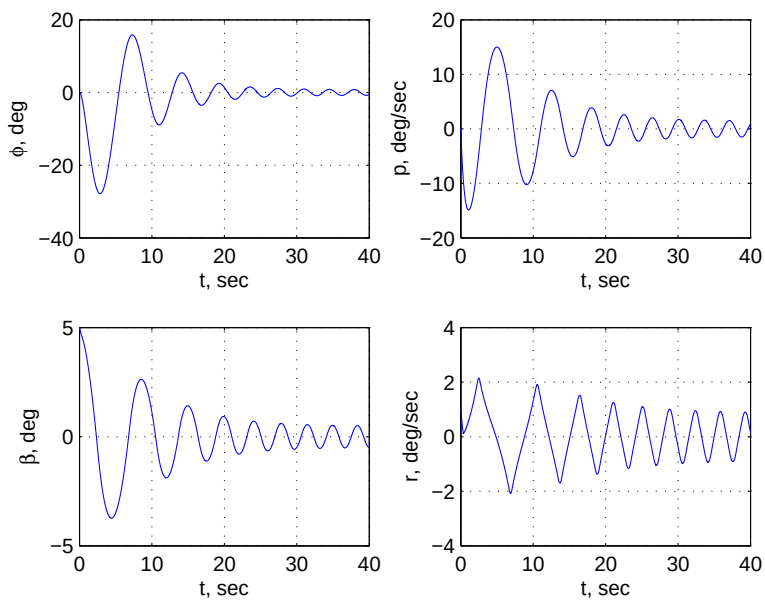

Fig. 18 - Response of GTM with 100% Break of Vertical Stabilizer at Mach 0.8 and 30K ft with Fast Engine Response ($\zeta = 0.024$, $\tau = 0.0518$ sec, $t_d = 0.3$ sec)

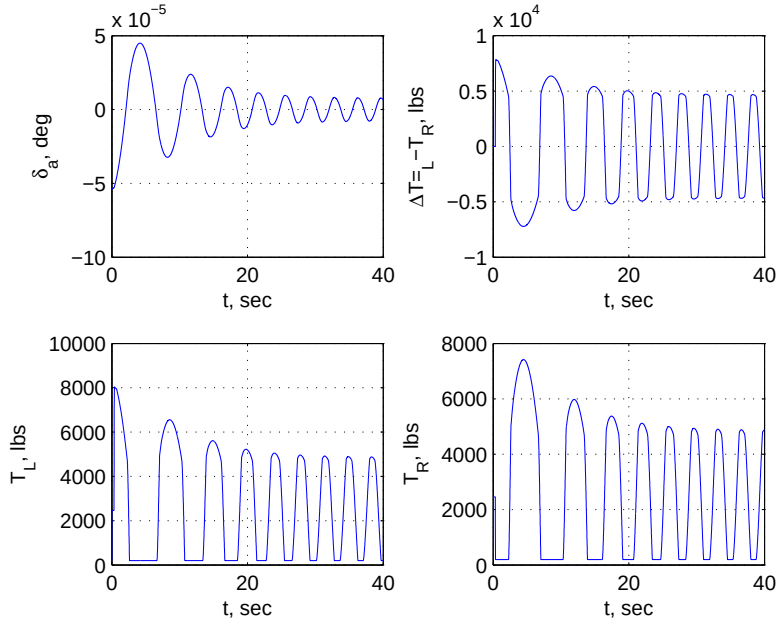

Fig. 19 - Aileron and Engine Thrusts for GTM with 100% Break of Vertical Stabilizer at Mach 0.8 and 30K ft with Fast Engine Response ($\zeta = 0.024$, $\tau = 0.0518$ sec, $t_d = 0.3$ sec)

VI. Conclusions

This paper presents an analysis of flight-propulsion control for a generic transport aircraft with failure scenarios that involve a disabled rudder system and damage to the vertical stabilizer. The engine dynamics are modeled as a time-delay second-order system based on a realistic nonlinear engine model. A yaw damper is designed for the flight-propulsion control to provide sufficient damping to the dutch roll mode in order to maintain aircraft directional stability. The analysis computes time constant and time delay requirements for aircraft engines to be used as control effectors in lieu of the rudder. In general, the dutch-roll damping tends to decrease with increasing airspeed and altitude. Also, the engine thrust decreases with increasing altitude. As a result, the engine response time requirements are more demanding for high speed and high altitude operations. At low airspeed and altitude, the engines have more thrust capability, so flight-propulsion control is more effective than at high airspeed and altitude. The initial conditions can play a role in stability of the flight-propulsion control due to the engine thrust saturation. As the airspeed and altitude increase, the limits on the roll and yaw rates can be quite small, so if the initial conditions on the roll and yaw rates exceed these limits, the aircraft will depart.

References

[1]National Transportation Safety Board, "In-Flight Separation of Vertical Stabilizer American Airlines Flight 587 Airbus Industrie A300-605R, N14053 Belle Harbor, New York, November 12, 2001", NTSB/AAR-04/04, 2004.

[2]National Transportation Safety Board, "United Airlines Flight 232 McDonnell-Douglas DC-10-10, Sioux Gateway Airport, Sioux City, Iowa, July 19, 1989", NTSB/AAR90-06, 1990.

[3]Lemaignan, B., "Flying with no Flight Controls: Handling Qualities Analyses of the Baghdad Event", AIAA Atmospheric Flight Mechanics Conference, AIAA-2005-5907, August 2005.

[4]Roskam, J., and Lan, C.-T. E., *Airplane Aerodynamics and Performance*, DARcorporation, 1997.

[5]Shah, G., "Aerodynamic Effects and Modeling of Damage to Transport Aircraft", AIAA Atmospheric Flight Mechanics Conference, AIAA-2008-6203, August 2008.

[6]Guo, T.-H., Litt, J., and Csank, J., "Simplified Engine Model", NASA Glenn Research Center, February 2009.

[7]Schmidt, L., *Introduction to AIrcraft Flight Dynamics*, AIAA, 1998.

[8]Nguyen, N., Ishihara, A., Krishnakumar, K., and Bakhtiari-Nejad, M., "Bounded Linear Stability Analysis - A Time Delay Margin Estimation Approach for Adaptive Control", AIAA Guidance, Navigation, and Control Conference, AIAA-2009-5968, August 2009.